Direct Measurement of Thermoelastic Properties of Glassy and Rubbery Polymer Brush Nanolayers Grown by "Grafting-from" Approach

M. Lemieux,[†] S. Minko,*,[‡] D. Usov,[‡] M. Stamm,[‡] and V. V. Tsukruk*,[†]

Materials Science & Engineering Department, Iowa State University, Ames, Iowa 50011, and Institut für Polymerforschung Dresden, Hohe Strasse 6, 01069 Dresden, Germany

We report the results of atomic force microscopy (AFM) based nanoscale probing of thermal and nanomechanical properties of relatively thick (50−90 nm) polymer brush layers from poly(styrene-*co*-2,3,4,5,6-pentafluorostyrene) (PSF) and polymethylacrylate (PMA). These layers, with a high density of grafting, are synthesized according to a "grafting-from" approach on a silicon surface modified with a reactive self-assembled monolayer. In the dry state, glassy and rubbery brush layers are found to be homogeneous matters with no signs of lateral chain segregation, which is observed for polymer layers with low to moderate grafting densities. We observed that thermal, mechanical, and thermoelastic properties of these polymer brush layers are virtually identical to that for unconfined polymers obtained concurrently via bulk polymerization. Direct measurement of heat dissipation and the thermoelastic response within the PSF brush layer confirms that the glass−rubber transition occurs between 100 and 110 °C as expected for the high-molecular weight polymer. Surface nanomechanical mapping reveals much lower adhesion of the PSF layer, which is glassy at room temperature and contains fluorine-enriched segments, in comparison with the sticky PMA layer containing polar segments. At room temperature, the PSF layer shows a compression elastic modulus of approximately 1 GPa whereas the rubbery PMA layer has an elastic modulus of 50 MPa, typical for the rubbery state. Heating the glassy PSF layer results in a gradual decrease of the elastic modulus caused by the glass transition, and conversion to the rubbery state is completed above 110 °C with an elastic modulus of 15 MPa.

Introduction

Polymer chains strongly tethered at one end to a surface, with a sufficiently high grafting density, act to alleviate overlapping by stretching away from the surface and forming a stretched conformation.[1−3] The resulting layer architecture, known as a polymer brush, has generated numerous theoretical and experimental investigations.[4−6] This situation, in which the polymer chains are stretched along the surface normal, is quite different from typical flexible polymer chain behavior in the isotropic amorphous bulk state, where the random-walk (Gaussian coil) configuration is found. Aside from the bulk state, the stretching of chains in the brush conformation is also very different for tethered polymer layers in which pancake and mushroom structures are found in the case when the grafting density is not high enough to induce chain crowding and overlapping. This stretching is considerably larger than the typical unstretched size of a chain, especially in the presence of a good solvent. The brush structure of these polymer layers is responsible for novel behavior and physical properties important for colloid stabilization,[7] drug delivery and biomimetic materials,[8,9]

chemical gates,[10] and tuning lubrication, adhesion, and wettability for tailored polymeric surfaces.[4,11,12]

Polymer brushes can be fabricated onto a substrate through both the "grafting-from" and "grafting-to" approaches.[5] The grafting-to approach involves preformed,[10] end-functionalized polymers reacting with a suitable surface under appropriate conditions to form a tethered polymer brush.[13−15] To facilitate the strong chemical attachment, the substrate is modified with a reactive precursor acting as a coupling agent, such as functionalized self-assembled monolayers (SAMs).[16,17] The grafting-to approach has one formidable drawback that becomes increasingly critical in the case of polymer brush layers: In general, only a small amount of polymer can be immobilized onto the surface by the grafting-to approach due to steric constraints and kinetic factors.[14] Reactive surface sites are quickly consumed, thus slowing diffusion of additional long macromolecular chains through the existing polymer film to reach the unreacted sites. Moreover, space constraints around potential reactive sites further limit the grafting density.[14,18,19] This barrier becomes even greater as the layer thickness increases.

* To whom correspondence should be addressed: e-mail minko@ipfdd.de or vladimir@iastate.edu.

† Iowa State University.

‡ Institut für Polymerforschung Dresden.

(1) Alexander, S. J. *J. Phys. (Paris)* **1977**, *38*, 977.

(2) de Gennes, P. G. *Macromolecules* **1980**, *13*, 1069.

(3) Milner, S. T. *Science* **1991**, *251*, 905.

(4) Halperin, A.; Tirrell, M.; Lodge, T. P. *Adv. Polym. Sci.* **1992**, *100*, 33.

(5) Zhao, B.; Brittain, W. J. *Prog. Polym. Sci.* **2000**, *25*, 677.

(6) Wittmer, J.; Johner, A.; Joanny, J. F. *Colloids Surf. A: Physiochem. Eng. Aspects* **1994**, *86*, 85.

(7) Pincus, P. *Macromolecules* **1991**, *24*, 2912.

(8) Galaev, I.; Mattiasson, B. *Trends Biotechnol.* **1999**, *17*, 335.

(9) Aksay, A.; Trau, M.; Manne, S.; Honma, I.; Yao, N.; Zhou, L.; Fenter, F.; Eisenberger, P. M.; Gruner, S. M. *Science* **1996**, *273*.

(10) Ito, Y.; Ochiai, Y.; Park, Y. S.; Imanishi, Y. *J. Am. Chem. Soc.* **1997**, *119*, 1619.

(11) Ruths, M.; Johannsmann, D.; Rühe, J.; Knoll, W. *Macromolecules* **2000**, *33*, 3860.

(12) Mansky, P.; Liu, Y.; Huang, E.; Russell, T. P.; Hawker, C. J. *Science* **1997**, *275*, 1458.

(13) Minko, S.; Patil, S.; Datsyuk, V.; Simon, F.; Eichorn, K. J.; Motornov, M.; Usov, D.; Tokarev, I.; Stamm, M. *Langmuir* **2002**, *18*, 289.

(14) Luzinov, I.; Julthongpiput, D.; Malz, H.; Pionteck, J.; Tsukruk, V. V. *Macromolecules* **2000**, *33*, 1043.

(15) Luzinov, I.; Julthongpiput, D.; Tsukruk, V. V. *Macromolecules* **2000**, *33*, 7629.

(16) Ulman, A. *Chem. Rev.* **1996**, *96*, 1533.

(17) Tsukruk, V. V.; Luzinov, I.; Julthongpiput, D. *Langmuir* **1999**, *15*, 3029.
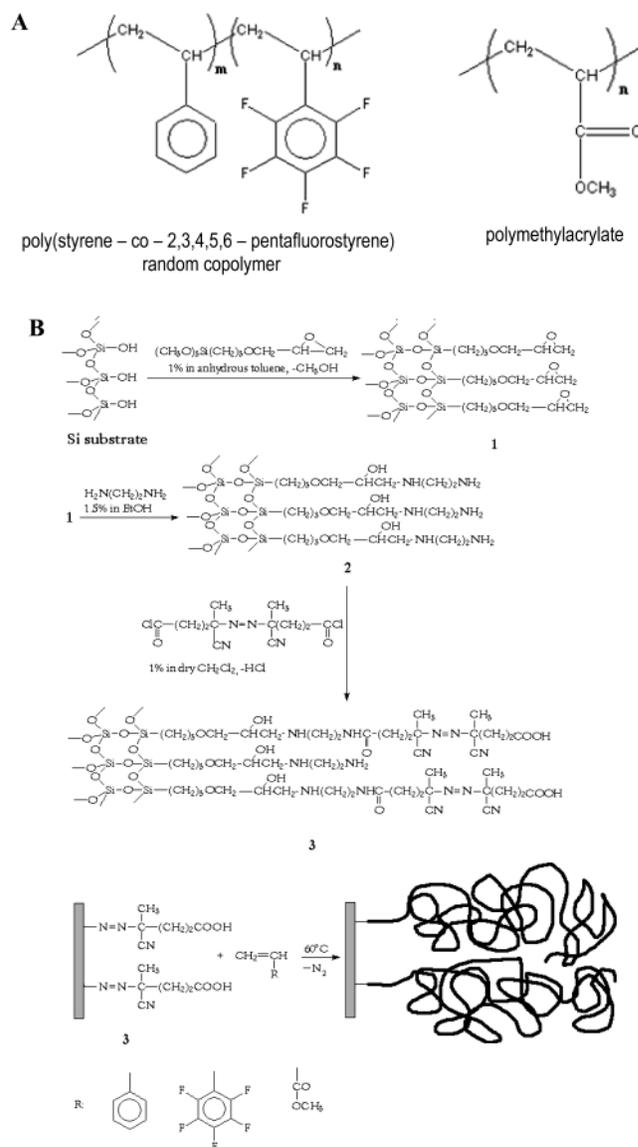
(18) Luzinov, I.; Julthongpiput, D.; Liebmann-Vinson, A.; Cregger, T.; Foster, M. D.; Tsukruk, V. V. *Langmuir* **2000**, *16*, 504.

Therefore, the amount of grafted polymer is usually in the range of 2−10 mg/m² (the total thickness of the brush layers is below 10 nm), although this still should be on the concentration edge to create the brush structure.[2,4,20]

To increase grafting density, radical polymerization *from* the substrate has been used in the past decade as an alternative method from the grafting-to approach for creating highly dense brushes of high molecular weight.[20−23] The grafting-from approach starts with the application of an immobilized radical initiator attached to the substrate via SAMs, followed by surface-initiated polymerization to form a tethered layer. Using this approach, some authors have reported high grafting densities in the range of 15−100 mg/m² and brush layer thickness on the order of 100 nm.[21,24−26]

The challenge for the grafting-from approach is a rather complicated synthesis involving several steps and requiring a high purity of the reaction mixture. Synthesis of polymers cannot be easily controlled, and molecular weight characteristics and actual experimentally determined physical properties of grafted polymer brush layers remain unknown. The preparation of densely grafted, uniform brushes remains a nontrivial task, and it has certainly hindered experimental studies in this area.[27] Additionally, once adequate synthesis is achieved, the physical properties remain unknown. In fact, very few experimental techniques are capable of directly measuring these properties, and thus, very few studies have even addressed this issue. The compression of physically and chemically grafted polystyrene brushes has been studied with the surface force apparatus and AFM.[11,28−30] It was found that the compression resistance of polymer brushes increases with increasing chain length and grafting density. However, in all these studies, the nanomechanical, thermoelastic, and thermal properties of brush layers directly measured remain unknown.

Therefore, in this work, we focus on the direct measurement of physical properties in different polymer brush layers. We conduct probing of the mechanical and thermal properties of glassy and rubbery brush layers and compare them with bulk properties of these materials, as well as with spin-coated bulk layers with similar thickness as the brush layers. To the best of our knowledge, this is the first attempt to quantify the mechanical and thermomechanical properties (Young's modulus, adhesion, glass transition temperature) of polymer brush layers. To accomplish this task, we use the combined capabilities of atomic force and scanning thermal microscopy techniques. The two brush layers presented in this study represent polymers with very different mechanical and thermal

(19) Prucker, O.; Naumann, C. A.; Rühe, J.; Knoll, W.; Franck, C. W. *J. Am. Chem. Soc.* **1999**, *121*, 8766.

(20) Sidorenko, A.; Minko, S.; Schenk-Meuser, K.; Duschner, H.; Stamm, M. *Langmuir* **1999**, *15*, 8349.

(21) Luzinov, I.; Voronov, A.; Minko, S.; Kraus, R.; Wilke, W.; Zhuk, A. *J. Appl. Pol. Sci.* **1996**, *61* (7), 1101.

(22) Minko, S.; Gafijchuk, G.; Sidorenko, A.; Voronov, S. *Macromolecules* **1999**, *32*, 4525.

(23) Minko, S.; Sidorenko, A.; Stamm, M.; Gafijchuk, G.; Senkovsky, V.; Voronov, S. *Macromolecules* **1999**, *32*, 4532.

(24) Boven, G.; Oosterling M. L. C. M.; Chall, G.; Schouten A. J. *Polymer* **1990**, *31*, 2377.

(25) Prucker, O.; Rühe, J. *Macromolecules* **1998**, *31*, 592.

(26) Prucker, O.; Rühe, J. *Macromolecules* **1998**, *31*, 602.

(27) Hu, T.; Wu, C. *Macromolecules* **2001**, *34*, 6802.

(28) (a) Klein, J. *Annu. Rev. Mater. Sci.* **1996**, *26*, 581. (b) Minko, S.; Usov, D.; Evgenij, G.; Stamm, M. *Macromol. Rapid Commun.* **2001**, *22*, 206.

(29) Butt, H. J.; Kappl, M.; Mueller, H.; Raiteri, R.; Meyer, W.; Ruhe, J. *Langmuir* **1999**, *15*, 2559.

(30) (a) Yamamoto, S.; Ejaz, M.; Tsujii, Y.; Matsumoto, M.; Fukuda, T. *Macromolecules* **2000**, *33*, 5602. (b) Yamamoto, S.; Ejaz, M.; Tsujii, Y.; Fukuda, T. *Macromolecules* **2000**, *33*, 5608.

Figure 1. (A) Structure of the polymers in PSF (upper left formula) and PMA (upper right formula) brushes. (B) Schematic representation of the synthetic route of brush fabrication: modification of Si wafer with GPS, the following treatment with ethylendiamine, attachment of Cl-ABCPA, and grafting-from growth.

properties, demonstrating that a wide range of adhesive to nonsticky polymer brushes can be synthesized and their physical properties can be quantitatively studied with the experimental procedures and approaches used in this research. It is clear that that these properties depend on chemical composition, molecular weight, and grafting density of the brush. Work is already underway in this lab for determining similar properties in glassy and rubbery polymers with different chemical compositions and molecular weights than used in this study. The aim of the present work was to determine and compare the thermoelastic response of highly dense, thick glassy and rubbery polymer brush layers.

Experimental Section

We synthesized specimens of two different polymer brushes of glassy (PSF) and rubbery (PMA) types (Figure 1a). The weight ratio of the random copolymer PSF is styrene:pentafluorostyrene = 0.75:0.25 as evaluated by NMR. Monomers of styrene (S) (Aldrich), 2,3,4,5,6-pentafluorostyrene (FS) (Fluka), and me-

thylacrylate (MA) (Aldrich) were purified on a chromatographic column. Initiators 4,4′-azobis(4-cyanopentanoic acid) (ABCPA) (Fluka) and 4,4′-azobis(isobutyronitrile) (AIBN) (Fluka) were purified by recrystallization from methanol. Toluene and tetrahydrofuran (THF) (Merck) of analytical grade were distilled after 1 h of boiling over sodium. (3-Glycidoxypropyl)trimethoxysilane (GPS) (ABCR GmbH, Karlsruhe, Germany), ethylendiamine (Acros Organics), and phosphorus pentachloride (Aldrich) were used as received.

The [100] silicon wafers were modified with GPS according to the previously described procedure[17,18] and afterward with 1.5% (wt) ethylendiamine in EtOH for 1.5 h. The acid chloride derivative of ABCPA (Cl-ABCPA) was prepared as described elsewhere.[24] The substrates were treated with a solution of 0.66 g of Cl-ABCPA and 0.36 mL of triethylamine in 50 mL of CH_2Cl_2 for 2 h (see the sketch in Figure 1b). Monomer solutions: (1) 73 g (0.70 mol) of S and 20 g (0.10 mol) of FS in 100 g of THF and (2) 50 g (0.58 mol) of MA in 50 g of toluene were cleaned by four freeze–pump–thaw cycles and recondensed to a reactor with added AIBN (4.36×10^{-4} mol/L). After the reactor was filled with Ar, four freeze–pump–thaw cycles were repeated. The Si wafers with the grafted azo initiator were placed under an Ar atmosphere in a glovebox into the reactor. The reactor was immersed into a water bath (60 ± 0.1 °C) for 12 h. After polymerization, the silicon wafers were rinsed several times with THF. The nongrafted polymer was removed by cold Soxhlet extraction in THF for a duration of 4 h.

Film thickness was measured by a Compel automatic ellipsometer (InOm Tech, Inc.) with the values of refractive indices determined for thick films according to the known procedure (for details see refs 14 and 18). This way, the thickness of a polymer layer can be determined within ±0.2 nm for homogeneous smooth layers. Since accurately determining the thickness is a critical step for the calculation of brush layer parameters, values found with ellipsometry were verified by an AFM scratch test. In this experiment, the polymer layer is scratched with an ultrasharp needle with enough force to delaminate the layer down to the Si wafer but not penetrate the Si wafer material. AFM imaging is then conducted over an area with the scribed line next to the unharmed polymer layer to verify quality of the scratch and actual thickness. In this study, both independent measurements conducted for 5–6 locations/specimen produced very consistent results with differences not exceeding 0.5 nm.

Bulk glass transition values determined with DSC measurements have been conducted on a Pyris 1 instrument (Perkin-Elmer). For this measurement, approximately 5 mg of bulk polymer was placed inside the sealed aluminum pod and heated from −30 to 50 °C (PMA) or from 20 to 150 °C (PSF). Chromatography analysis of solution-grown polymers was completed on a Breeze 1500 instrument (Waters) with polystyrenes as calibration standards.

Spin-coated PMA and PSF physisorbed layers were made to represent PMA and PSF polymer layers in which the chains are in the random coil conformation found in the bulk state. The polymers were dissolved in good solvents (toluene for PSF and acetone for PMA) and spin-coated onto bare Si wafers. The coating speed (3000 rpm) and number of drops (6–10) were optimized to produce bulk layer thicknesses that exactly matched the brush layer thicknesses, in order that direct comparisons could be made between the two states. Contact angle measurements were conducted with a sessile drop method on a custom-made system.

The surface morphology and nanomechanical properties of the dry polymer brush layers under ambient conditions have been studied with the Dimension 3000 and the Multimode atomic force microscopes (AFM) (Digital Instruments, Inc., Santa Barbara). Silicon or silicon nitride tips with radius of 20–50 nm were used with spring constants of tips ranging from 0.01 to 50 N/m. Tapping-mode AFM was used according to the well-established procedure adapted in our lab.[31] Scan rates were usually 0.5–2 Hz, and exerted forces did not exceed several nanonewtons in imaging mode. Force volume mode, which utilizes the collection of the force–distance curves (FDC) over selected surface areas, was used for micromechanical analysis (MMA) of polymer brush layers. A single FDC records the forces acting on

the tip as it approaches and retracts from a point on the sample surface.[32] Force volume mode allows for the micromapping of the mechanical properties of polymer surfaces with nanometer-scale resolution, while obtaining topographical information simultaneously.[33,34] Typically, we used 64×64 pixels within $1 \times 1\ \mu m$ surface areas to micromapping with a lateral resolution of 15 nm. Force volume experiments at elevated temperatures were conducted in the DI thermal stage sample holder. Data collected were processed with an MMA software package developed in our lab, which provides means for calculation of localized elastic modulus, depth profile of elastic modulus, reduced adhesive forces, and surface histograms of elastic moduli and adhesive forces from experimental images as described elsewhere.[35] Spring constants of cantilevers were determined from resonant frequencies and the tip-on-tip method according to the procedures described earlier.[36,37] Tip radii were evaluated with scanning of reference gold nanoparticle specimens and a deconvolution procedure.[38,39]

Scanning thermal microscopy (SThM) with microthermal analysis (μTA) mode was used for independently testing the thermal properties of the PSF layer. Routines have been developed that allow this technique to be applicable to thin polymer films.[40,41] SThM was interfaced with an Explorer microscope (Thermomicroscopes). The thermal probe was a Wollaston microwire (90% Pt, 10% Rd) that formed a sensing loop with an effective radius of curvature of about 5 μm and resistance of 2.8–3.5 ohms. Thermal probes were calibrated with a poly(ethylene terephthalate) reference sample with well-known thermal transitions. The values of glass transition temperature (measurements were technically limited to the temperature interval of 25–450 °C) were determined from heat dissipation data in accordance with the procedure discussed in detail earlier.[42]

Results and Discussion

Chemical Composition and Surface Morphology. The thickness and grafting density of the polymer brush layers were controlled by terminating the reaction after 12 h. For these studies, we chose a grafting amount of approximately 50 mg/m² for PMA and 90 mg/m² for PSF that is typical for the grafting-from approach.[20] The thickness of the polymer layers measured independently with ellipsometry and with AFM scratch test was about 50 nm for the PMA layer and 87 nm for the PSF layer (Table 1). These values are much higher than typical grafting densities and thicknesses that can be achieved by the grafting-to technique. The molecular weights (M_w and M_n) determined from GPC for the PSF and PMA obtained concurrently via bulk polymerization under identical conditions have values of 629 000 and 556 000 (g/mol), respectively (Table 1). The polydispersity of each polymer is quite modest and close to the expected value (1.90 for PMA and 1.58 for PSF). The molecular weight of these polymers can serve as a guide for the evaluation of the anticipated molecular weight for grafted brushes

(31) Tsukruk, V. V. *Rubber Chem. Technol.* **1997**, *70*, 430.

(32) Cappella, B.; Dietler, G. *Surf. Sci. Rep.* **1999**, *34*, 1.
(33) *Scanning Probe Microscopy of Polymers*; Ratner, B., Tsukruk, V. V., Eds.; ACS Symposium Series; American Chemical Society: Washington, DC, 1998; Vol. 694.
(34) *Microstructure and Microtribology of Polymer Surfaces*; Tsukruk, V. V., Wahl, K., Eds.; American Chemical Society: Washington, DC, 1999; Vol. 741.
(35) (a) Tsukruk, V. V.; Gorbunov, V. V. *Probe Microsc.* **2002**, *3-4*, 241. (b) Tsukruk, V. V.; Huang, Z.; Chizhik, S. A.; Gorbunov, V. V. *J. Mater. Sci.* **1998**, *33*, 4905.
(36) Hazel, J. L.; Tsukruk, V. V. *Thin Solid Films* **1999**, *339*, 249.
(37) Hazel, J. L.; Tsukruk, V. V. *J. Tribol.* **1998**, *120*, 814.
(38) Radmacher, M.; Tillmann, R. W.; Gaub, H. E. *Biophys. J.* **1993**, *64*, 735.
(39) Tsukruk, V. V.; Gorbunov, V. *Microsc. Today* **2001**, *01–1*, 8.
(40) Gorbunov, V. V.; Fuchigami, N.; Hazel, J. L.; Tsukruk, V. V. *Langmuir* **1999**, *15*, 8340.
(41) (a) Gorbunov, V. V.; Fuchigami, N.; Tsukruk, V. V. *Probe Microsc.* **2000**, *2*, 53. (b) Gorbunov, V. V.; Fuchigami, N.; Tsukruk, V. V. *Probe Microsc.* **2000**, *2*, 65.
(42) Tsukruk, V. V.; Gorbunov, V. V.; Fuchigami, N. *Thermochim. Acta* **2003**, *395*, 241.

Table 1. Characteristics of Polymers and Polymer Brush Layers

	M_w (g/ mol)	M_w/M_n	T_g (°C)	contact angle (°)	layer thickness (nm)	elastic modulus (MPa)	reduced adhesive forces (N/m)
spin-coated bulk PSF layer	629 000	1.58	108[a]	95	NA	1200−1600	0.24
spin-coated bulk PMA layer	556 000	1.90	5[a]	79	NA	7−10	NA
PSF brush layer	NA	NA	109	99	87	1000−1200	0.37
PMA brush layer	NA	NA	NA	84	50	50−60	1.95

[a] Indicates data derived from macro DSC measurement on bulk volume polymer, not thin spin-coated layer.

Table 2. Geometrical Parameters of Grafted Macromolecules

	grafted amount (mg/m²)	grafting density (chains/nm²)	grafting distance (nm)	h_Θ (nm)	$2R_g$ (nm)
PSF brush layer	90	0.138	3.0	43	36
PMA brush layer	50	0.126	3.2	30	30

under assumption of close correlation of the grafted polymers and the bulk polymers.[22]

Thus, the anticipated grafting density (D, chains/nm²) of the brush layers was evaluated from M_n and the layer thickness (d, nm) according to the formula $D = d\rho N_a/(M_n \times 10^{21})$, where ρ (g/cm³) is density of the polymer and $N_a = 6.022 \times 10^{23}$ (mol^{-1}) is Avogadro's number.[14] The end-to-end distance (h_Θ, nm) of an unperturbed polymer chain in bulk state was calculated from $h_\Theta = kM_n^{0.5}$, where k was taken to be 0.070 for PSF and 0.068 for PMA. The radius of gyration, R_g, was calculated from $h_\Theta/\sqrt{6}$ (Table 2).[43] Grafting density was estimated to be greater than 0.1 chain/nm², which is high for these very long-chain macromolecules. Indeed, the anticipated average distance between grafting points, l, calculated as $l = 2(\pi D)^{-0.5}$, was close to 4 nm for both polymers, which is an indication of high grafting density (Table 2). Considering a geometrical size of the macromolecules of 30−43 nm, we can conclude that more than 100 chains are strongly overlapped within a volume occupied by a single grafted macromolecular chain. In addition, even in the dry state, significant stretching is expected for the PSF brushes where the layer thickness was 2 times larger than the macromolecular diameter and modest stretching (60%) is anticipated for rubber PMA macromolecules (Table 2).

Tapping-mode AFM in the "light tapping" regime was used to characterize the brush morphologies in the dry state. Prior to scanning, the samples were exposed to good solvents (toluene for PSF, acetone for PMA) for roughly 1 h that act to swell the brushes. They were then dried very quickly under dry N_2 inside clean-room conditions. Even in the dry state (bad solvent conditions), grafted layers for both polymers were uniform with homogeneous chemical composition as indicated by concurrent topographical and phase imaging obtained at different scales (Figures 2 and 3). Random variations of layer thickness on a submicrometer scale were very modest with resulting microroughness within 1×1 μm surface areas not exceeding 0.3−0.6 nm. The latest value is close to the cross-sectional dimensions of a single polymer chain and is a characteristic of molecularly smooth surfaces. This is in contrast with polymer layers with low to moderate grafting densities, for which lateral inhomogeneities and domain microstructure are frequently observed.[5,44] Experimental and theoretical studies have shown that in bad solvent conditions (such as air in this case) a polymer brush will collapse into dimples or clusters with sizes

dependent upon the grafting density. However, in the case of ultrahigh density of grafting, even in bad conditions, the brush will collapse into a homogeneous layer, bypassing the pinned micelle and dimple states.[45-47] Apparently, a much higher grafting density and high molecular weight of the polymers resulted in a higher level of overlapping of macromolecular chains and a truly uniform surface morphology.

Elastic Properties of Polymer Brush Layers. Force-volume testing of dry polymer brush layers gives direct insight into their mechanical properties. Initially, micromapping of both polymer layers conducted under identical conditions confirmed a homogeneous layer composition (Figure 4). Micromapping of 1×1 μm surface areas with lateral resolution of 15 nm showed uniform elastic response and adhesive force distributions throughout the probed area, except for surface defects. The value of the compressive elastic modulus represented by a gray level for identical images is much higher for the glassy polymer layer (Figure 4). Correspondingly, the level of adhesive forces is much higher for the rubbery polymer layer. The difference in the adhesiveness of the two brushes arises from two contributions: the fact that one is glassy and the other rubbery at ambient conditions, and the presence of fluorinated groups (PSF) versus nonfluorinated PMA. The exact level of each contribution to the difference in adhesive forces will be the subject of future tests.

Respective histograms of surface distribution calculated from these images confirmed these conclusions and provided for quantitative characterization of the interfacial thermoelastic properties (Figure 5). In fact, these histograms demonstrate narrow distribution of the nanomechanical response, with random deviations of elastic moduli and reduced adhesive forces not exceeding 16% and 11%, respectively, for the entire surface area tested (Figure 5). These are characteristics of excellent uniformity in chemical composition and microstructure. The absolute values of the elastic moduli are scattered in the range of 1000−1200 MPa for the PSF layer, which contrasts sharply with 50−60 MPa for the PMA layer. The PSF value is close to typical values measured for thin layers of glassy polymers, and the PMA value is typical for rubbery polymer phases.[48] Moreover, the values for PSF brush layers are fairly close (slightly below but still within experimental uncertainty) to the experimental values determined for spin-coated films of corresponding poly-

(43) *Polymer Handbook*, 4th ed.; Brandrup, J., Immegurt, E. H., Grulke, E. A., Eds.; John Wiley & Sons: New York, 1999.

(44) (a) Kelley, T. W.; Schorr, P. A.; Johnson, K. D.; Tirrell, M.; Frisbie, C. D. *Macromolecules* **1998**, *31*, 4297. (b) Karim, A.; Tsukruk, V. V.; Douglas, J. F.; Satija, S. K.; Fetters, L. J.; Reneker, D. H.; Foster, M. D. *J. Phys. II* **1995**, *5*, 1441.

(45) Koutos, V.; van der Vegte, E. W.; Hadziioannou, G. *Macromolecules* **1999**, *32*, 1233.

(46) Siqueira, D. F.; Kohler, K.; Stamm, M. *Langmuir* **1995**, *11*, 3092.

(47) Zhulina, E. B.; Birshtein, T. M.; Priamitsyn, V. A.; Klushin, L. I. *Macromolecules* **1995**, *28*, 8612.

(48) Chizhik, S. A.; Huang, Z.; Gorbunov, V. V.; Myshkin, N. K.; Tsukruk, V. V. *Langmuir* **1998**, *14*, 2606.
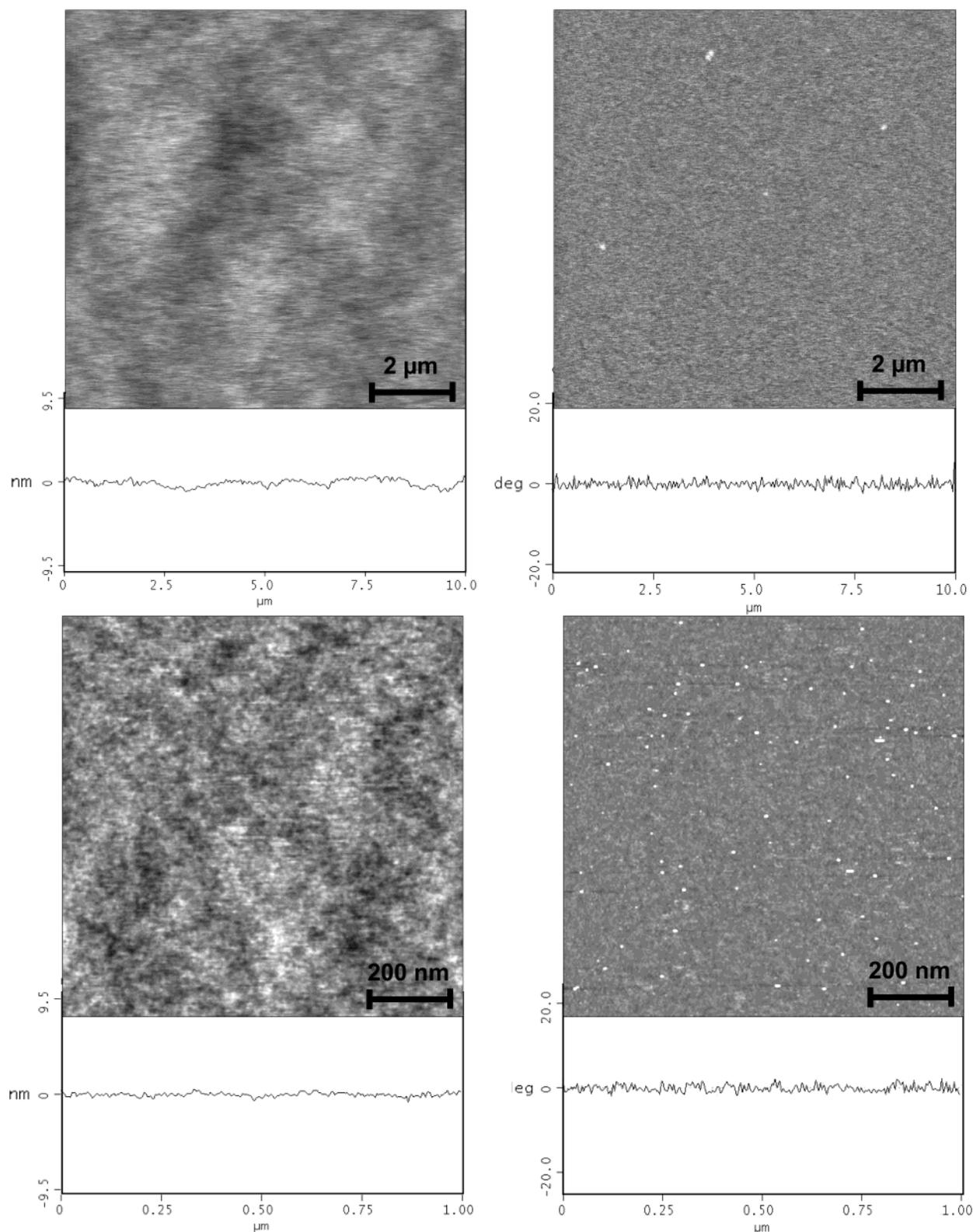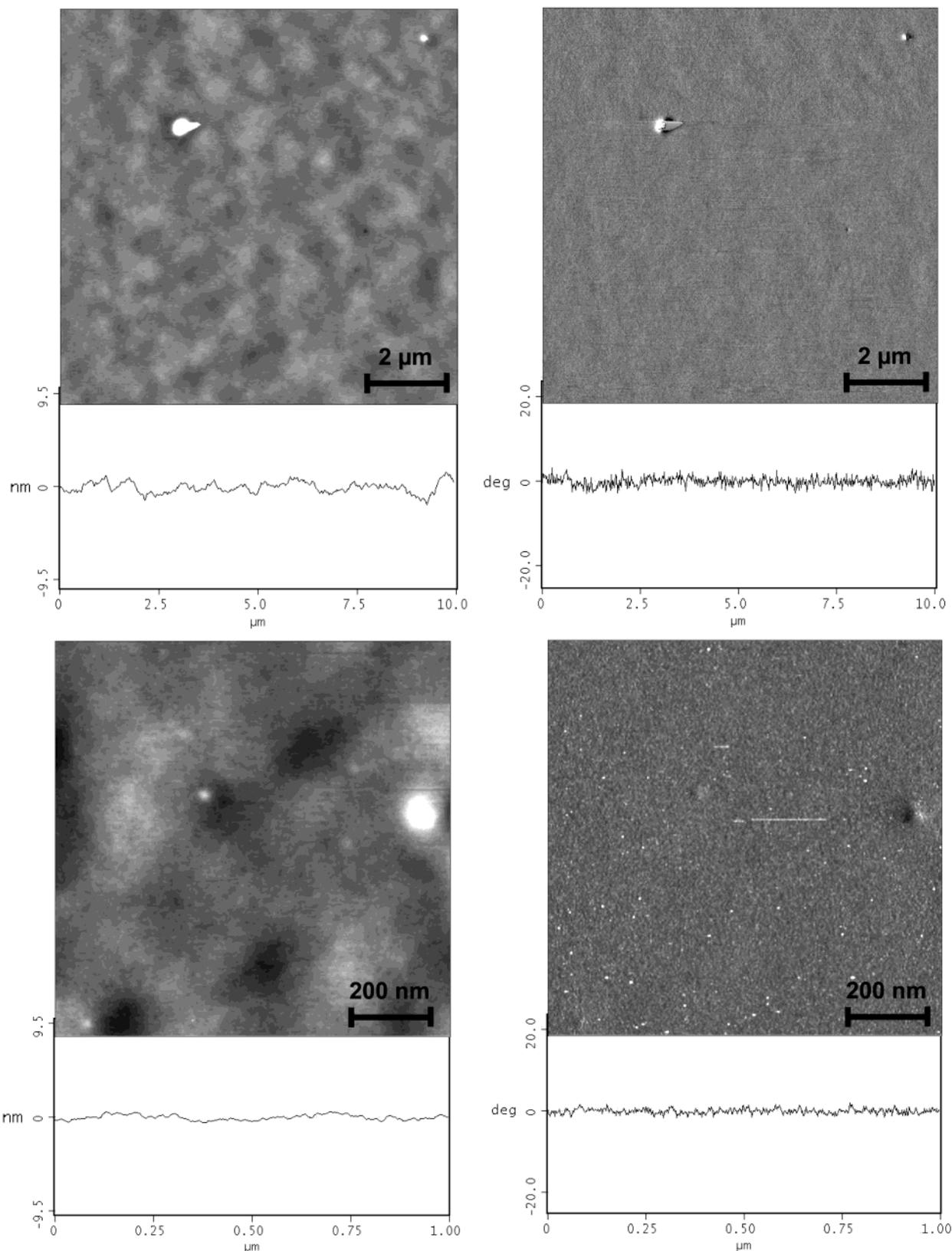
Figure 2. AFM images (left, topography; right, phase) of the PSF layer at 10×10 μm (top) and 1×1 μm (bottom). Height z-scale is 10 nm and scale for phase is 50°. Occasional bumps observed were external impurities. Corresponding cross-sections are included for topography and phase to illustrate the uniformity in topography and chemical composition.

mers obtained via bulk polymerization as well as polystyrene (Table 1). Therefore, direct AFM measurements confirm truly glassy and rubbery states of PSF and PMA brush layers, respectively.

Analysis of force−distance curves reveals that PSF and PMA layers have very different surface properties, with much higher adhesion observed for the PMA layer during the retracting cycle of the tip (Figure 6). The difference between the approaching and retracting curves at the point the tip "snaps" out of the physical contact with the sample gives an indication of the total energy needed to fully withdraw the AFM tip, and this difference is clearly much larger with PMA then with PSF (Figure 6). The reduced adhesive force, defined as the pull-off force normalized to

Figure 3. AFM images (left, topography; right, phase) of the PMA layer at 10 × 10 μm (top) and 1 × 1 μm (bottom). Height z-scale is 10 nm and scale for phase is 50°. Occasional bumps observed were external impurities. Corresponding cross-sections are included for topography and phase to illustrate the uniformity in topography and chemical composition.

the tip radius R, $\Delta F/R$, is essentially a measure of adhesive energy required to separate the AFM silicon tip and polymer surface.[33,34] These values, calculated from force volume data, are much higher (more than 5 times) for the rubbery layer (Figure 5, Table 1). This results from the

physical distinction, as well as differences in chemical composition at the surfaces of the brush layers. With a high concentration of fluoro-containing groups, PSF has a substantially lower surface energy then PMA, where polar double bonds contribute to high surface energy in
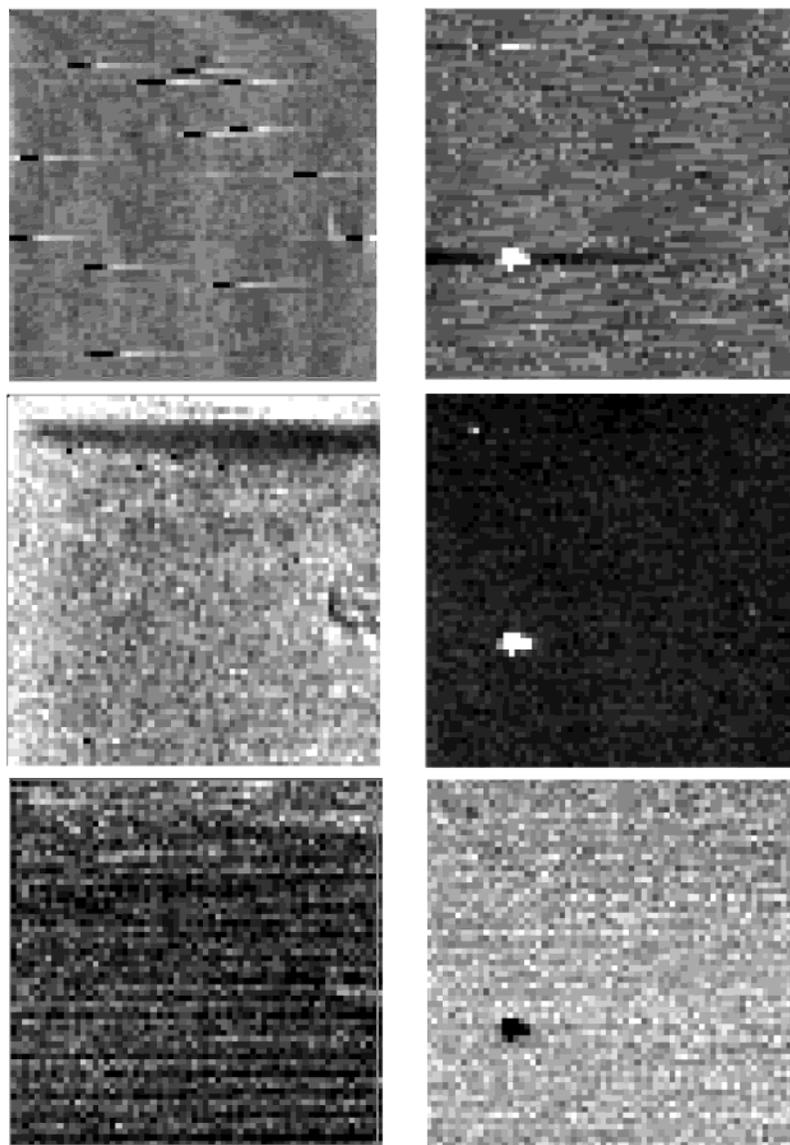
Figure 4. Force volume images with $64 \times 64 \times 64$ resolution at 1×1 μm. The images represent topography (top row), elastic modulus distribution (middle row), and pull-off force distribution (bottom row). The left column is for PSF while the right is for PMA. The z-scale is identical for both specimens and, thus, brightness represents a relative level for these two samples (brighter = higher level).

the rubbery material.[49,50] Additionally, as is known for AFM experiments, the pull-off force is affected by a difference in the mechanical contact area between the AFM tip and the layer surface, which is higher for the more compliant rubbery PMA layer.[34,51] The larger contact area during the retracing cycle affects the total forces required to disjoint the tip−surface contact.

Another important feature of the force−distance curves is the slope of the approaching curve. This slope shows how an actual deflection of the AFM cantilever progresses with the surface indentation. A slope nearing unity indicates an extremely stiff surface such as on a silicon surface, and smaller values reflect larger surface indentation.[34,52] The approaching curve slope is noticeably different for PSF than for PMA (Figure 6). The slope is

much higher for the PSF layer and varies from 0.6 to 0.8 for PSF as compared to 0.2−0.4 for PMA. This implies much more compliant behavior of the PMA layer.

Indeed, conversion of the force−distance curves to indentation−load curves underlines different microme-chanical response of glassy and rubbery layers (Figure 7a). Apparently, under identical normal load, the pen-etration of the AFM tip is much higher (5−10 times) for the rubbery PMA layer. The rubbery PMA layer supports a much lower normal load than the glassy PSF layer. Direct calculations of the depth profile of the elastic modulus showed much higher absolute values for the PSF layer (Figure 7b). The absolute values of the elastic modulus for the PSF brush are close but slightly lower than that for spin-coated PSF and polystyrene films (Figure 7b). In addition, lower indentation depths are achieved for the PSF layer under similar normal loads. Typically, the

(49) Mason, R.; Jalbert, C. A.; O'Rourke Muisener, P. A. V.; Koberstein, J. T.; Elman, J. F.; Long, T. E.; Gunesin, B. Z. *Adv. Colloid Interface Sci.* **2001**, *94*, 1.

(50) Israelachvili, J. *Intermolecular and Surface Forces*; Academic Press: San Diego, CA, 1992.

(51) Johnson, K. L. *Contact Mechanics*; Cambridge University Press: Cambridge, U.K., 1985.

(52) (a) Luzinov, I.; Julthongpiput, D.; Bloom, P. D.; Sheares, V. V.; Tsukruk, V. V. *Macromol. Symp.* **2001**, *167*, 229. (b) Chizhik, S. A.; Gorbunov, V. V.; Fuchigami, N.; Luzinov, I.; Tsukruk, V. V. *Macromol. Symp.* **2001**, *167*, 169.
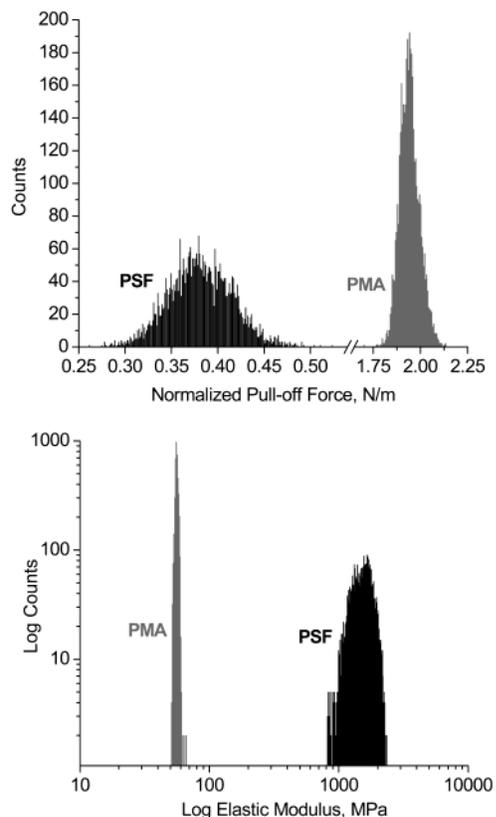
Figure 5. Histograms comparing the micromechanical mapping data for PMA and PSF layers. The contrast in modulus and adhesion (pull-off force) values is detected for PSF and PMA. All histograms are taken from $64 \times 64 \times 64$ force volume scans, giving a total of 4096 data points. The modulus represented here is the average modulus for full penetration into the layer. The pull-off force data were normalized to the tip radius.
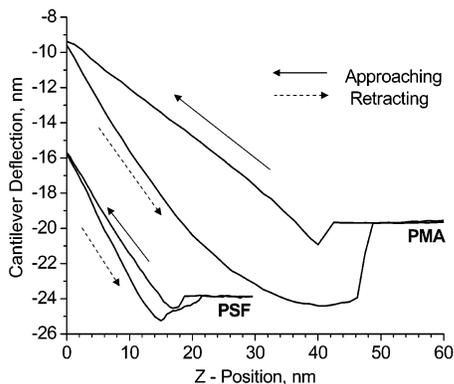
Figure 6. Typical force−distance curves for PSF and PMA layers. Note the difference in slope of the approaching curves and the large hysteresis in the retracting mode between the glassy and rubbery brush layers. Curves are offset for clarity.

maximum indentation depth under the normal load of 60 nN was within 25−30 nm for the rubbery PMA brush layer but only 6−8 nm for the PSF brush layer.

Generally, data for particular indentation depths and particular location are scattered around a virtually constant level for both layers. Under certain probing conditions, a tendency toward higher values at smaller indentation depths was observed, but this phenomenon may be associated with the viscoelastic phenomenon and requires additional investigations. It is worth noting that, under the loading conditions exploited here, the radius of the mechanical contact estimated from force−distance
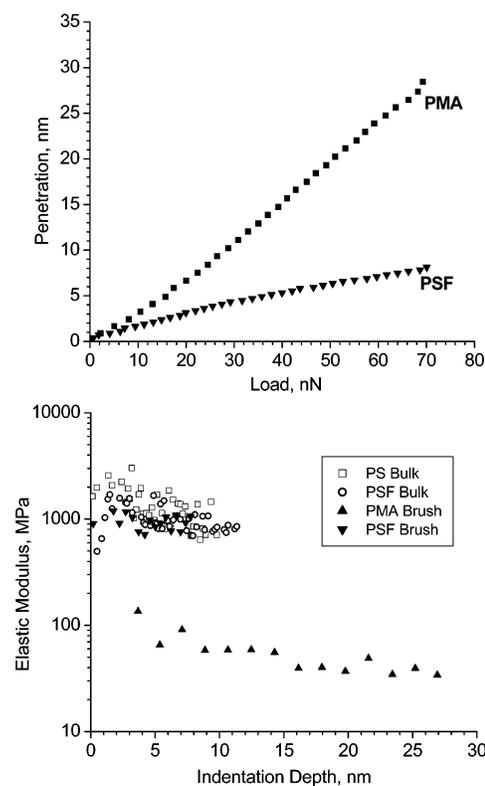

Figure 7. (A, top panel) Penetration−load curves for PMA and PSF layers. At equal normal loads, a significantly larger penetration took place into the more compliant PMA layer. (B, bottom panel) Elastic modulus depth profiles for PSF and PMA layers. Results are also shown for PS and PSF bulk samples, which are spin-coated films. The thickness of the spin-coated samples is the same as for the respective grafted brush layers.

curves by Hertzian mechanics according to the known relationships varies from 5 nm (for lower load) to 9 nm (highest load).[45,48,53] Considering that the anticipated dimensions of the macromolecules are close to 40 nm (Table 2), we can conclude that mechanical probing was confined to surface areas much smaller than a dimension of a single macromolecular chain. Thus, our results confirm that on a spatial scale finer than macromolecular chains, PSF and PMA brushes are indeed homogeneous materials with elastic properties of glassy and rubbery bulk polymers, respectively.

Thermal Mechanical Properties of Polymer Brush Layers. The thermoelastic properties of the brush layers were examined through independent measurements with μTA and force volume measurements at elevated temperatures. μTA measurements of heat dissipation for the PSF brush layer allowed direct evaluation of the glass transition temperature (PMA layer with $T_g = 5\ °C$ was not measured because of technical constraints limiting the temperature range to those above room temperature) (Figure 8). Several independent measurements at different surface locations demonstrated the presence of singularities in heat dissipation at temperatures around 108−110 °C. The glass transition temperature determined from these data was 109 °C, which is close to the glass transition temperature obtained from the DSC experiment on bulk-polymerized PSF specimen (Table 1). This can be considered as a strong indication that PSF within the brush layer retains the thermal properties of the bulk polymer with high molecular weight. Further studies of thermo-

(53) (a) Tsukruk, V. V. *Adv. Mater.* **2001**, *13*, 95. (b) Tsukruk, V. V.; Shulha, H.; Zhai, X. *Appl. Phys. Lett.* **2003**, *82*, 907.
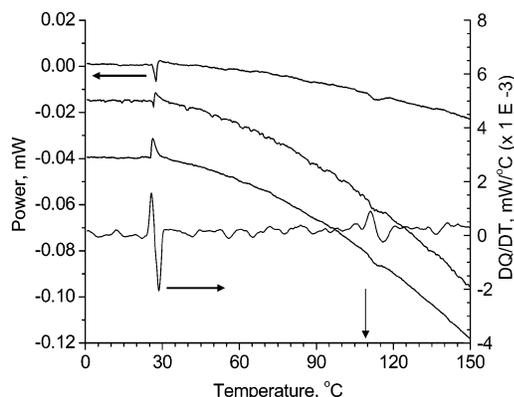
Figure 8. μTA measurements on the PSF layer: the power dissipation data (left scale) for different locations are compared with a single-derivative curve (right scale) from the data. At this thickness, a glass transition can be clearly seen around the 110 °C mark. Heating rate was 5 °C/s. Power scale is offset to clearly show all curves.
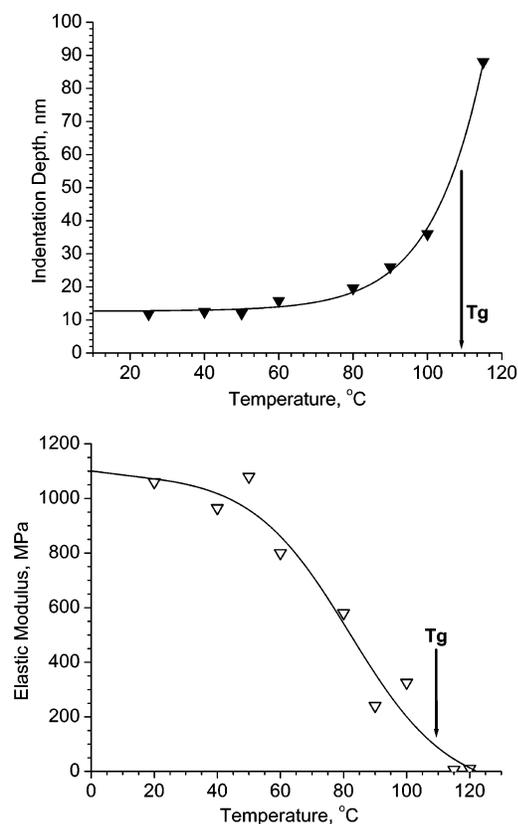
Figure 9. (A) Penetration depth for the PSF layer at different temperatures with identical normal load at each temperature. Above the glass transition, full penetration through the 87 nm thick layer was achieved. (B) Temperature variation of the elastic modulus for the PSF layer.

mechanical properties of the PSF brush layer via force volume measurements at elevated temperature confirm this conclusion (Figure 9).

As we observed, the maximum indentation depth achievable under identical normal loads at different temperatures was virtually constant and close to 10 nm for temperatures below 60 °C (Figure 9a). At higher temperatures, the compliance of the PSF brush layer increased gradually. A sharp rise of the indentation depth was observed for temperatures above 90 °C. This indicates a sharp increase of polymer compliance associated with the unfreezing of segments and increased mobility in the

course of glass transition. The elastic modulus, calculated from force–volume data at elevated temperatures, showed the thermomechanical behavior typical for amorphous polymers (Figure 9b). It remains virtually unchanged for temperatures below 60 °C and then drops dramatically (50 times) to 15 MPa for temperatures above 110 °C. This thermomechanical behavior corresponds to that expected for bulk PSF polymer with a glass transition temperature of 108 °C. The transition is somewhat wide (ranging from 60 to 110 °C), but not unusual for high molecular weight, amorphous glassy polymers with broad molecular weight distribution.[54,55]

Conclusions

In conclusion, we exploited AFM-based techniques for probing of the thermal and mechanical properties of thick (50–90 nm) polymer brush layers synthesized according to the grafting-from approach. As we observed, both glassy (PSF) and rubbery (PMA) brush layers were extremely homogeneous entities with no indications of lateral segregation, which is usually observed for brush layers with lower grafting densities. All thermal, mechanical, and thermoelastic properties of polymer brush layers studied here were *directly measured* with nanoscale resolution for the first time. As we observed, they were close to those for unconfined polymers obtained via bulk polymerization under identical conditions. This points out that an undisturbed composition and microstructure of polymers grown from a reactive silicon surface by the grafting-from technique.

Micromapping of the surface mechanical properties revealed much lower adhesion of the PSF layer enriched with fluorine-containing segments and much higher surface stiffness in comparison with the complaint PMA layer containing polar double-bond segments. Differences in both the contact areas and chemical interactions can be held responsible for this phenomenon. At room temperature, an elastic modulus of approximately 1 GPa was determined for the glassy PSF brush. The rubbery PMA layer possesses the elastic modulus typical for the reinforced rubber state (about 50 MPa). Heating the glassy PSF layer resulted in a gradual decrease of the elastic modulus completed by full conversion to the rubbery state with the elastic modulus close to 15 MPa, indicating glass transition behavior of a typical bulk, high molecular weight polymer. *Direct measurement* of heat dissipation and thermoelastic response within the PSF brush layer independently with high-temperature AFM and SThM techniques confirmed that the glass–rubber transition occurs between 100 and 110 °C as expected for a bulk, unconfined polymer. To the best of our knowledge, this is the *first direct measurement* of thermoelastic properties of grafted-from polymer brush layers on a nanoscale. This work proves that the brush film possess physical properties that are, in fact, close to those for high-molecular weight materials obtained via bulk polymerization.

(54) Van Krevelen, D. W. *Properties of Polymers*; Elsevier: Amsterdam, 1997.
(55) Gorbunov, V. V.; Fuchigami, N.; Luzinov, I.; Tsukruk, V. V. *High Perform. Polym.* **2000**, *12*, 603.